

Effects of Environmentally Induced Asymmetries on Hurricane Intensity: A Numerical Study

LIGUANG WU

*Goddard Earth and Technology Center, University of Maryland at Baltimore County, Baltimore, and Laboratory for Atmospheres, NASA
Goddard Space Flight Center, Greenbelt, Maryland*

SCOTT A. BRAUN

Laboratory for Atmospheres, NASA Goddard Space Flight Center, Greenbelt, Maryland

(Manuscript received 15 April 2003, in final form 2 June 2004)

ABSTRACT

The influence of uniform large-scale flow, the beta effect, and vertical shear of the environmental flow on hurricane intensity is investigated in the context of the induced convective or potential vorticity asymmetries in the core region with a hydrostatic primitive equation hurricane model. In agreement with previous studies, imposition of one of these environmental effects weakens the simulated tropical cyclones. In response to the environmental influence, significant wavenumber-1 asymmetries develop. Asymmetric and symmetric tendencies of the mean radial and azimuthal winds and temperature associated with the environment-induced convective asymmetries are evaluated. The inhibiting effects of environmental influences are closely associated with the resulting eddy momentum fluxes, which tend to decelerate tangential and radial winds in the inflow and outflow layers. The corresponding changes in the symmetric circulation tend to counteract the deceleration effect. The net effect is a moderate weakening of the mean tangential and radial winds. The reduced radial wind can be viewed as an anomalous secondary radial circulation with inflow in the upper troposphere and outflow in the lower troposphere, weakening the mean secondary radial circulation.

1. Introduction

Asymmetries that develop in tropical cyclones (TCs) have been extensively studied for decades (e.g., Simpson 1952; Jordan 1952; Shea and Gray 1973; Lewis and Hawkins 1982; Jorgensen 1984; Gall et al. 1998; Kuo et al. 1999; Reasor et al. 2000). Recently, the dynamics of the asymmetries in the TC inner core region have been investigated in a series of studies that focused mainly on tropical cyclogenesis using a barotropic asymmetric balance model (Möller and Montgomery 1999), a three-dimensional (3D) quasigeostrophic model (Montgomery and Enagonio 1998), a 3D asymmetric balance model (Möller and Montgomery 2000), and a shallow-water model (Enagonio and Montgomery 2001). These adiabatic studies examined the impact of potential vorticity (PV) sources and sinks associated with deep convection and demonstrated that convectively induced asymmetries in the core region can accelerate the tangential wind through vortex axisymmetrization (Melander et al. 1987; Montgomery and Kallenbach 1997).

Other sources of asymmetries are related to influences of the large-scale environment. Recent numerical studies suggest that weakening of simulated TCs is closely associated with these environmentally induced asymmetries that develop in the vicinity of the TC eyewall. Using full-physics numerical models, Peng et al. (1999) and Frank and Ritchie (1999, 2001) investigated TC intensity change due to large-scale environmental influences (e.g., the beta effect, uniform environmental flows, and vertical shear of the environmental flow) and showed that, if one of these environmental factors is included in numerical experiments, the resulting vortex is weaker than the one without environmental influence. Peng et al. (1999) suggested that separation of the surface flux maximum and the lateral moisture convergence reduces precipitation and inhibits the development of the simulated TCs in their model. On the other hand, Frank and Ritchie (2001) argued that in the upper troposphere TC asymmetries induced by environmental shear become sufficiently strong that air with high values of potential vorticity and equivalent potential temperature are mixed outward rather than into the TC eye. As a result, the warm core aloft weakens and the central pressure begins to rise. These results suggested that the responses of a TC to environmentally induced asym-

Corresponding author address: Dr. Liguang Wu, NASA GSFC, Code 912, Greenbelt, MD 20771.
E-mail: liguang@agnes.gsfc.nasa.gov

metries can be quite different from that associated with purely convectively generated asymmetries.

Chen et al. (2003) recently suggested that TC asymmetries can decelerate the mean tangential wind in the vicinity of the radius of maximum wind (RMW). They applied the theory of empirical normal modes to the study of inner spiral bands formed in a simulated hurricane using the nonhydrostatic fifth-generation Pennsylvania State University–National Center for Atmospheric Research Mesoscale Model (MM5). The resulting Eliassen–Palm (EP) flux divergence for the leading asymmetric modes, which is proportional to the change of the mean tangential wind resulting from the eddy effects, indicates that the combined effects of the wavenumber-1 and -2 modes (their Fig. 11) lead to a deceleration tendency in the tangential wind at lower and upper levels in the vicinity of the RMW, while the acceleration tendency primarily occurs in lower and middle levels slightly inside the RMW. Chen and Yau (2003) further investigated the development of asymmetric structures in an explicitly simulated landfalling hurricane and found that the asymmetric structures tend to counteract the effect of the mean circulation.

Eddy fluxes of heat and momentum associated with the large-scale circulation can contribute to the symmetric circulation of TCs. During the formative stage, as shown by Pfeffer (1958), Challa and Pfeffer (1980), and Challa et al. (1998), large-scale environmental eddy fluxes can induce a secondary radial circulation with outflow in the upper troposphere and inflow in the lower troposphere, thereby drawing moisture into the region, organizing the convection, and providing lifting necessary to set off conditional instability. Molinari and Vollarro (1990) evaluated the contributions of eddy fluxes to investigate the vertical structure of the interaction of Hurricane Elena (1985) with a baroclinic wave. Bosart et al. (2000), Persing et al. (2002), and Möller and Shapiro (2002) investigated the rapid intensification of Hurricane Opal (1995) in terms of the eddy fluxes of heat and momentum associated with an approaching trough with varying assessments of the impacts.

The objective of this study is to understand the underlying physical processes responsible for the weakening of TCs that occurs when they are subjected to simple environmental influences, similar to those examined by Peng et al. (1999) and Frank and Ritchie (1999, 2001). The effects of environment-induced TC asymmetries will be examined in the context of the associated eddy flux in a series of idealized numerical experiments with a full-physics model. The results are qualitatively similar to those of Chen et al. (2003) since both studies assess the eddy fluxes associated with spiral rainbands. In this study, however, the link between environmental influences, spiral bands, and their weakening effects on TCs is established. The asymmetries are associated with highly idealized large-scale flows and not with large-scale circulations such as troughs and the asymmetries result from the interaction be-

tween those environmental influences and the TC circulation.

This paper is organized as follows. In section 2, we summarize the numerical model used in this study and the numerical experiments. Section 3 describes the response of TCs to the imposed environmental influences, including both the symmetric and asymmetric structure. In section 4, the contributions of the resulting asymmetric circulations to the TC intensity change are evaluated. In section 5, physical mechanisms associated with the environmental influences are discussed based upon the results in this study. Conclusions are provided in section 6.

2. Numerical model and experimental design

In previous studies, the numerical models used were diverse in terms of their resolution and the complexity of the model physics. For example, the horizontal grid spacings used by Peng et al. (1999) and Wu (1999) were 0.5° and 25 km, respectively, whereas the simulations by Frank and Ritchie were performed with a grid spacing of 15 km in 1999 and 5 km in 2001. Peng et al. and Wu used the Kuo scheme (Kuo 1974) for cumulus physics, while Frank and Ritchie applied the cumulus parameterization of Betts and Miller (1986) to their 15-km simulations and an explicit moisture scheme to their 5-km experiments. The simulated responses of TCs to imposed large-scale flows were generally similar in all of these experiments. Therefore, the first-order effects of the environmental flows are phenomena that can be qualitatively simulated in a numerical model with relatively coarse resolution and simple physics.

In this study, the numerical model is the same as that used by Wu and Wang (2000). Cumulus convection is parameterized with Kuo's (1974) cumulus scheme and the calculations of horizontal and vertical turbulent fluxes of momentum, heat, and moisture follow Smagorinsky et al. (1965) and Louis (1979), respectively. No dissipative heating is included. The details of the model and its capability in simulating the motion and evolution of baroclinic TCs in the presence of diabatic heating are documented by Wu and Wang (2000, 2001a,b). The model consists of 201×201 grid points with a uniform horizontal spacing of 25 km and 16 vertical layers.

This study examines four numerical experiments that are designed to investigate the various environmental factors: the planetary vorticity gradient (beta effect), uniform zonal environmental flow, and vertical shear of the mean zonal flow. All the experiments begin with the same initially symmetric baroclinic vortex. The tangential wind profile of the initial cyclonic vortex is shown in Fig. 1a, with a maximum wind of 25 m s^{-1} at a radius of 100 km. The sea surface temperature (SST) is horizontally uniform and fixed (29.5°C) throughout the integration. The first experiment (E0) is a control run on an f plane without environmental flow. In agreement

with Wu and Wang (2000), the vortex does not move and maintains its symmetric structure throughout the integration period of 96 h. Using Emanuel's (1988) approach,¹ the maximum potential intensity (MPI) in terms of the central pressure and maximum wind speed are 897.5 mb and 68.9 m s^{-1} , respectively. The simulated central pressure and maximum wind were 901.5 mb and 66.0 m s^{-1} at 90 h, slightly weaker than, but close to, the MPI. The simulated storm is able to nearly attain its MPI since the simulation neglects the weakening effects of parameterized downdrafts, vertical shear, and other feedbacks. As shown in Fig. 1b, the RMW tilts outward slightly with height and a warm core of about 10°C develops at about 250 mb. The maximum wind appears near the top of the boundary layer (900 mb) because of surface friction. In general, the model produces a simulated TC with relatively realistic general structure.

As shown in Table 1, the other three experiments are performed under the influence of vertical shear of the zonal environmental wind (E1), the beta effect (E2), and uniform zonal mean flow (E3), respectively. The large-scale environmental influence is imposed at the beginning of the integration. The imposed wind, consisting of either mean zonal flow or vertically sheared flow, can significantly affect the TC structure and even prevent development from occurring if the flow or shear is excessively strong. Therefore, we select a moderate uniform flow of -4 m s^{-1} in E3 and a moderate vertical shear associated with winds that decrease with height from -4 m s^{-1} at the surface to 0 m s^{-1} at the top of the model in E1.

3. Response to environmental effects

a. TC intensity

Figure 2 shows the evolution of the maximum wind at the lowest model level and the central pressures for all of the simulations. The run with zero-mean flow (E0) is the most intense simulation. All simulated TCs develop in a similar manner. That is, the first 36 h of rapid intensification is followed by a period of slower intensification and finally by a quasi-steady state. The major changes in TC intensity associated with the different large-scale environments are most evident after 36 h of integration, although their influence is imposed at 0 h. Such a delayed response of the storm's intensity was noticed by Frank and Ritchie (2001) using the nonhydrostatic MM5 fifth-generation mesoscale model.

In E1, the vortex reaches a central surface pressure of 910.6 mb at 96 h. Compared with case E0, the central surface pressure increases by about 8 mb and the maximum wind decreases by about 4 m s^{-1} as a result of

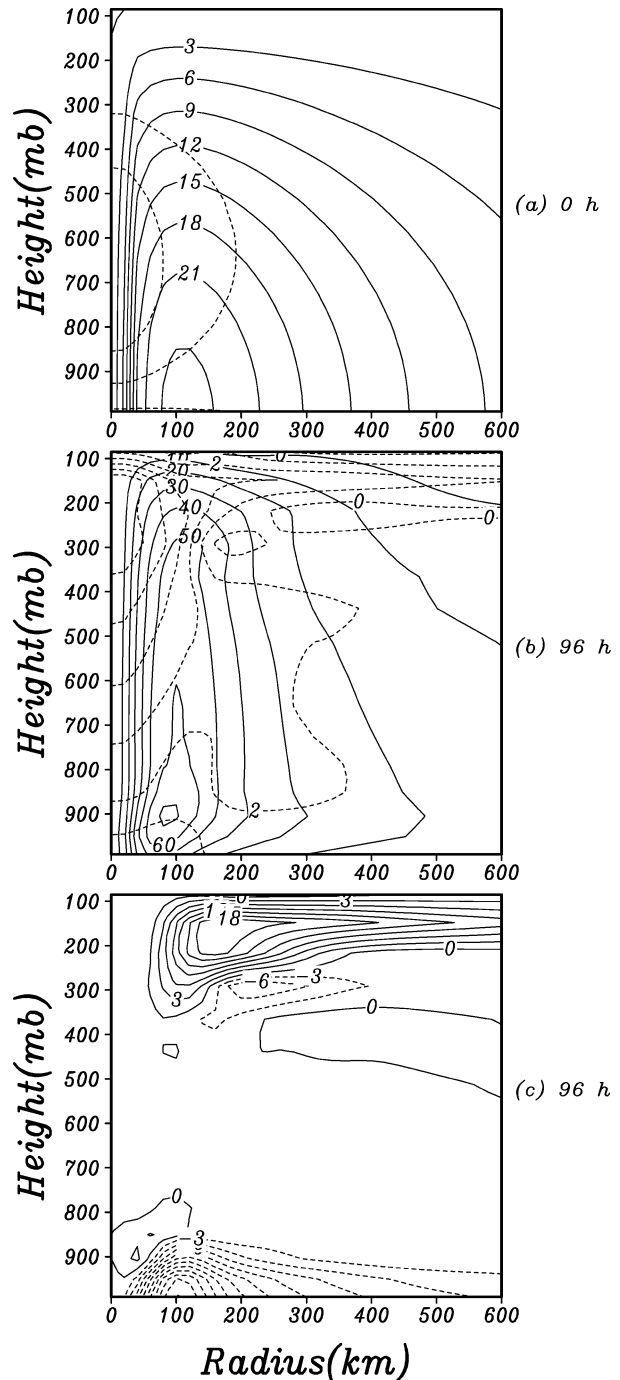


FIG. 1. Tangential winds (solid) and temperature anomalies (dashed) with respect to the environment in E0 at (a) 0 h and (b) 96 h, and (c) radial winds at 96 h. The intervals are 2°C for the temperature anomaly, 3 m s^{-1} in (a) and (c) and 10 m s^{-1} in (b) for winds.

the imposed vertical shear of the environmental flow. Case E2 is run on a beta plane without environmental flow. The vortex only attains a central surface pressure of 937.2 mb and maximum wind of 52 m s^{-1} at 96 h, a pressure rise of about 35 mb and velocity decrease of

¹ The value of C_k/C_d , where C_k is the enthalpy exchange coefficient and C_d is the momentum drag coefficient, is approximately 0.7 for the Louis (1979) parameterization.

TABLE 1. Summary of the numerical experiments.

| Experiment | Environmental flow | Plane | Heating |
|------------|--------------------|---------|----------|
| E0 | NA | f | Diabatic |
| E1 | Sheared | f | Diabatic |
| E2 | NA | β | Diabatic |
| E3 | Uniform | f | Diabatic |

14 m s⁻¹ compared to E0. In E3, with a uniform easterly environmental flow of -4 m s⁻¹, the storm's intensity is reduced by about 21 mb and 9 m s⁻¹ at 96 h. Consistent with the study of Peng et al. (1999), introduction of either uniform zonal environmental flow, vertical shear of the zonal environmental flow, or the beta effect weakens the TCs.

Frank and Ritchie (2001) found that in a similar easterly flow simulation the storm was slightly more intense than the zero-flow case. They argued that although significant asymmetries developed in the eyewall structure in their easterly flow case, the evaporation of rainfall and resolvable-scale downdrafts, which were simulated in their model, made the boundary layer cooler in their zero-flow case because the storm did not move. This process is included in neither the current study nor the study by Peng et al. (1999) since downdrafts are not included in the cumulus parameterization.

b. Symmetric structure

In the following analysis, the TC circulation is decomposed into its azimuthally symmetric and asymmetric components. In this study, the vortex center is defined as that which maximizes the symmetric tangential wind (Reasor et al. 2000). In order to determine the storm center, a variational approach is used to adjust the location of the center until the maximum azimuthal mean wind speed is obtained. The TC center location is only determined at the lowest model level. Because of the moderate environmental effects, the variation of the center location with height is typically within a grid size (25 km) of the surface center from the surface to 300 mb.

Careful examination of the structures of the simulated TCs indicates that they are significantly modified by the imposed moderate environmental influences. Despite the coarse horizontal resolution, the RMW shifts outward slightly in response to the large-scale environmental effects. Figure 3 shows the deviations of the symmetric tangential wind in each case from E0 at 96 h. The decrease in the tangential wind extends through all levels in E2 and E3, mainly just inside of the RMW. Note that the shift of the RMW cannot account for the wind reduction because negative values generally extend to a radius of 200 km, well beyond the RMW. In E1, the reduction of the tangential wind occurs primarily at upper levels. Note that a relatively smaller reduction (E2 and E3) or even increase (E1) in the mean tangential

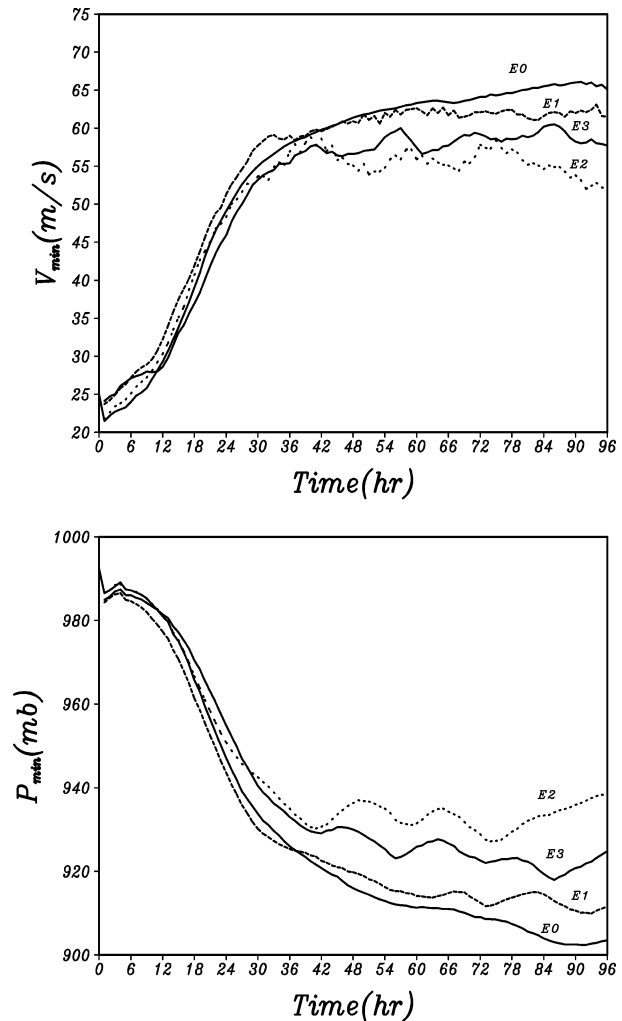


FIG. 2. Time series of (top) maximum wind at the lowest model level and (bottom) minimum central pressures for cases E0, E1, E2, and E3.

wind appears around 700–800 mb in the vicinity of the RMW. This feature will be discussed in the next section.

Consistent with the structure of a mature hurricane, inflow and outflow in case E0 are located primarily in the lower and upper layers, as shown in Fig. 1c. A secondary inflow maximum can be found at about 300 mb. Figure 4 shows the deviations of the symmetric radial wind in E1, E2, and E3 from that in E0 at 96 h. As a result of the environmental influences, the outflows in the upper layer are significantly reduced in E2 and E3, and slightly reduced in the 100–200-mb layer in E1. In addition, inflow in the boundary layer in E2 and E3 is also reduced. The positive anomalies around 300 mb in Fig. 4 are associated with the weakening of the secondary inflow maximum there. The reduction in both the inflow and outflow indicates a weakening of the symmetric radial circulation.

Figure 5 shows the temperature anomalies with respect to the environment at 96 h. The magnitudes of

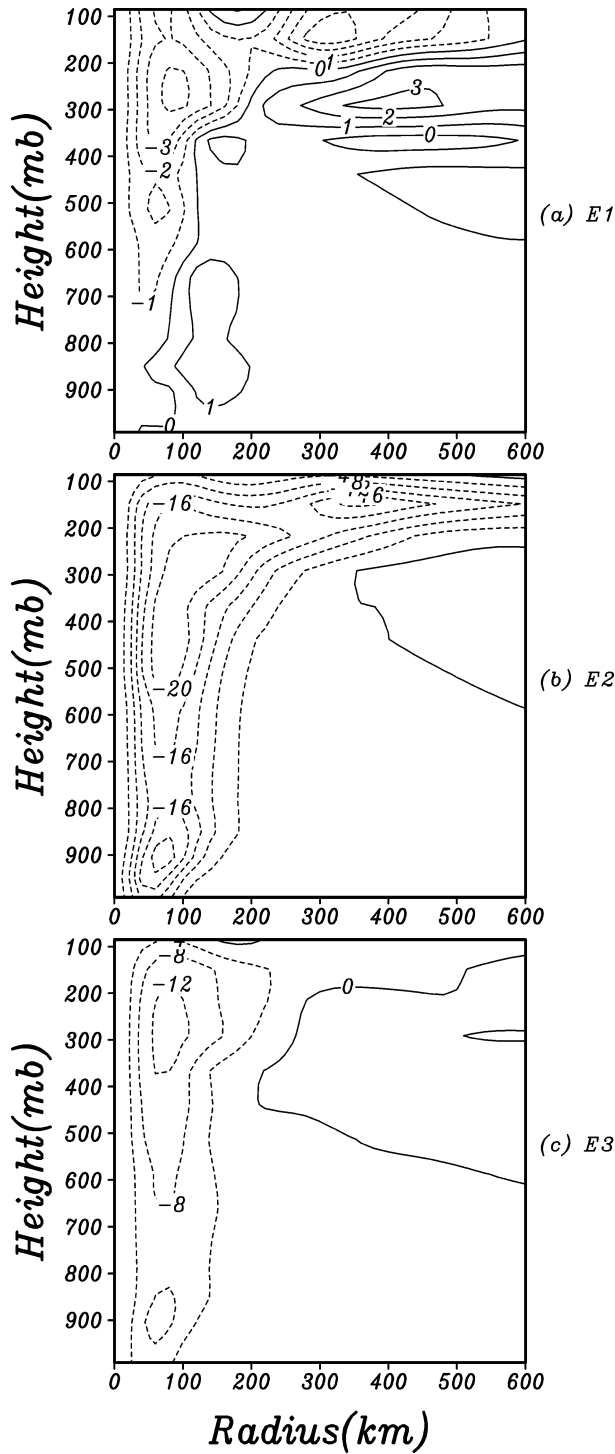


FIG. 3. Deviation of the tangential wind in (a) E1, (b) E2, and (c) E3 from that in E0 at 96 h. The intervals are 1 m s^{-1} in (a) and 4 m s^{-1} in (b) and (c).

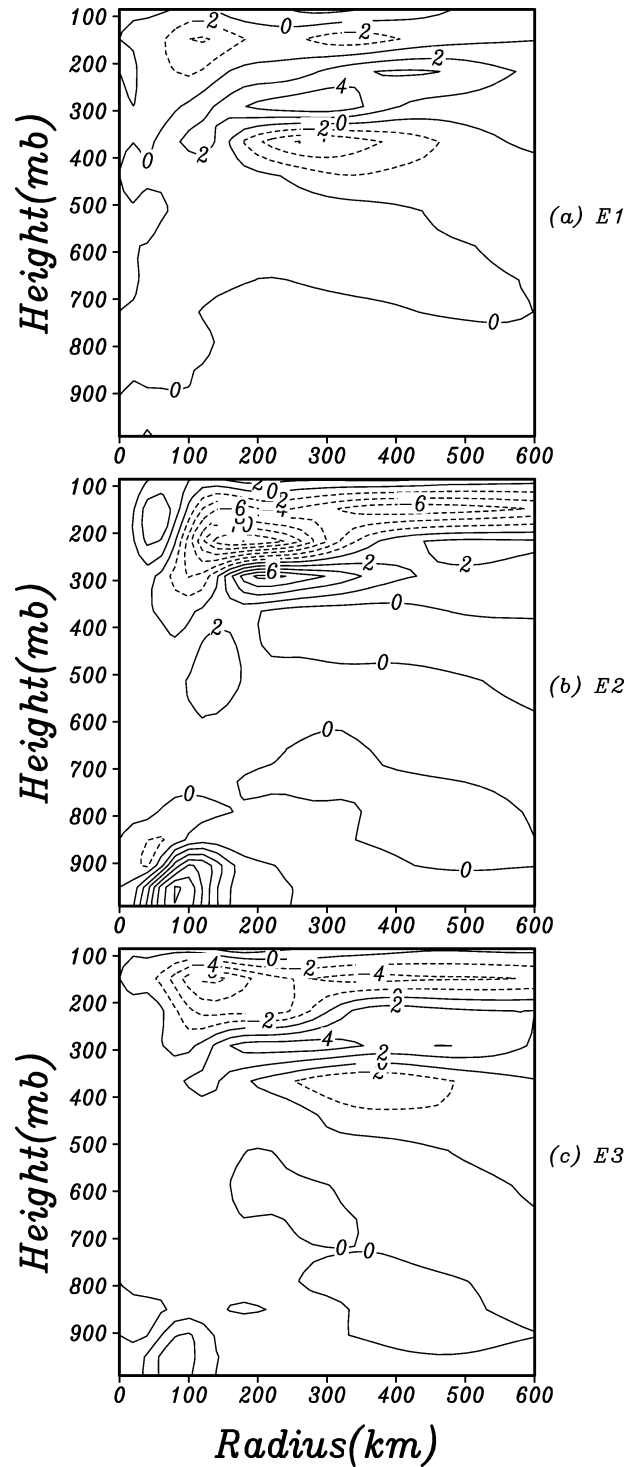


FIG. 4. Deviation of the radial winds in (a) E1, (b) E2, and (c) E3 from that in E0 at 96 h. The intervals are 2 m s^{-1} .

the maximum temperature anomalies are almost the same in all the experiments (about 12°C). However, the heights of the warm cores are generally lower than in E0 (Fig. 1b) as a result of the weakening effects

of the specified environments. The warm cores are located around 250 mb in E0 and E1, whereas they are located at about 350 mb in E3 and 450 mb in E2. Consistent with hydrostatic balance, the lowest cen-

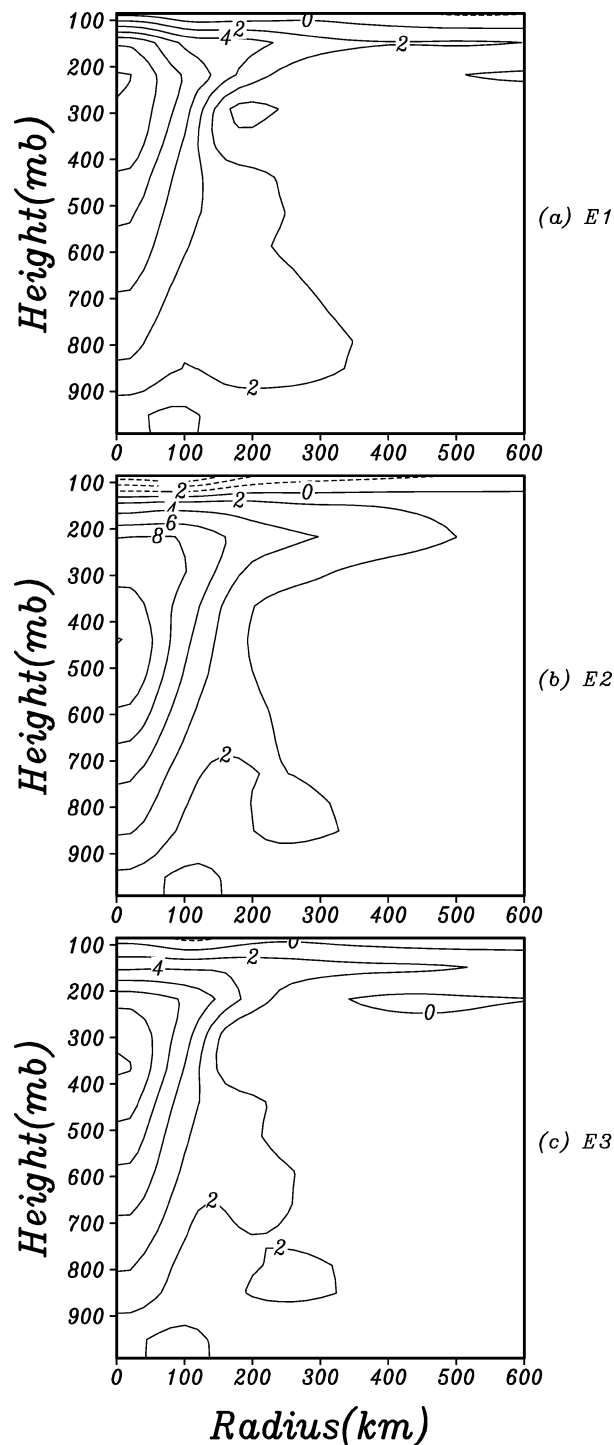


FIG. 5. Temperature anomalies relative to the environment in (a) E1, (b) E2, and (c) E3 at 96 h. The intervals are 2°C .

tral pressures are found in cases where the warm anomalies are located at the highest heights. Thus, Fig. 5 suggests that, compared to E0, the reduced intensities in E2 and E3, as measured by the minimum central pressure, are associated with a lowering of the

warm anomaly and are not so much a result of a reduction in its magnitude.

c. Asymmetric structure

A common feature in the three experiments (E1, E2, and E3) is the significant asymmetry that develops as a result of the imposed environmental effects. Figure 6 shows the evolution of the asymmetries in terms of potential vorticity (PV) at level 14 (900 mb) for E1, E2, and E3. May and Holland (1999) and Chen and Yau (2001) found that local maxima of PV are closely associated with convective asymmetries since latent heat release is the main process leading to PV generation. Figure 7 shows the asymmetric vertical motion fields at level 585 mb (negative values are upward) for E3. Comparison of this figure with Fig. 6 (lower panels) clearly indicates that positive PV bands are regions with upward vertical motion. For this reason, the PV asymmetries are used as a proxy for enhanced convection. As indicated by the small circles in Fig. 6, after the initial development stage (12 h), the asymmetries indicated by PV maxima show both leading and trailing spiral structures. Willoughby et al. (1984) provide a schematic diagram of radar reflectivity in TCs that includes convective structures outside of the core and shows that high reflectivity in the eyewall extends outward cyclonically. In this sense, the resulting PV anomaly patterns in Fig. 6 bear a remarkable resemblance to the spiral bands observed in real hurricanes.

Several mechanisms associated with the generation of TC asymmetries have been discussed in previous studies. Shapiro (1983) suggested that asymmetries in surface friction caused by vortex translation tend to produce a wavenumber-1 asymmetry in convergence, in which the maximum eyewall convergence occurs ahead and to the right of the storm motion vector for slow to moderate moving TCs. Jones (1995) showed that the tilt of a TC can lead to significant asymmetric structure of TCs because of balance requirements. Peng et al. (1999) investigated the development of TC asymmetries in the context of the surface frictional wind. In the presence of an easterly flow, for example, the tangential wind on the northern side and the inward radial wind on the eastern side of the vortex are increased. As a result, an easterly flow is expected to generate maximum surface flux in the northeastern part of the vortex. In the presence of environmental wind shear, convection tends to be enhanced on the downshear-left side (Frank and Ritchie 1999, 2001; Reasor et al. 2000).

These mechanisms can operate simultaneously in the present cases. For example, since the TC in E1 moves slowly westward, Shapiro's mechanism may be responsible for the positive PV anomaly that occurs to the west of the TC center. In E1, the westerly environmental shear may contribute to the positive PV anomaly on the northern side. These asymmetries are primarily generated by the environmental influences.

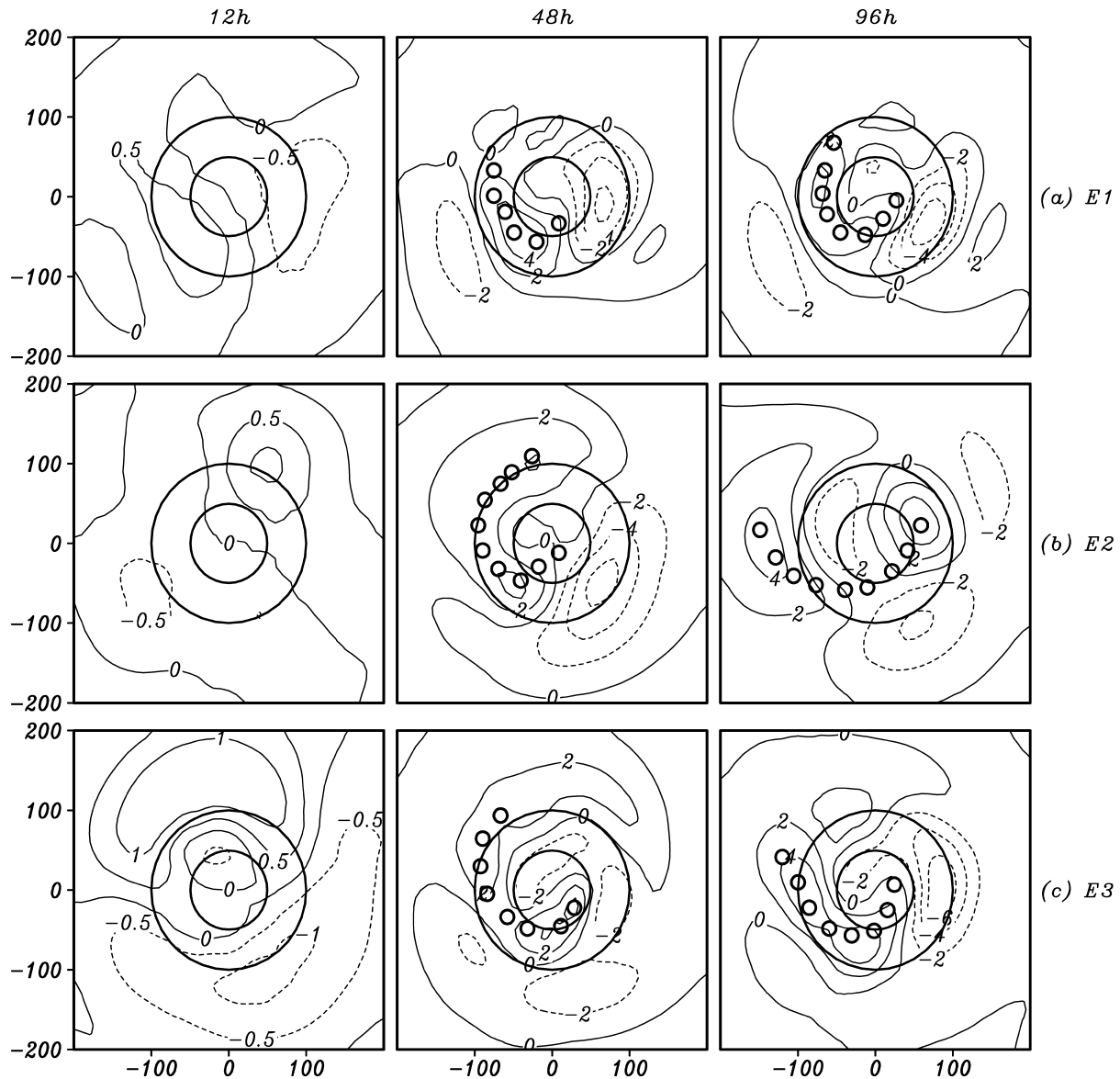


FIG. 6. Asymmetric PV components at 900 mb after 12-, 48-, and 96-h integration in (a) E1, (b) E2, and (c) E3, respectively. The unit for PV is PVU ($10^{-6} \text{ K m}^2 \text{ kg}^{-1} \text{ s}^{-1}$). The radii of the two circles are 50 and 100 km, respectively. Small circles denote the axis of the PV maximum.

4. Asymmetric contribution to intensity change

Eliassen's (1952) symmetric balanced formulation has been used to understand the influence of eddy fluxes associated with the large-scale circulation on the formation and intensification of hurricanes (Pfeffer 1958). The contributions of eddy fluxes of heat and momentum are thereby related to the deduced secondary radial circulation. In this dynamical framework, a hurricane is treated as a stable symmetric vortex that never deviates far from hydrostatic or gradient balance. Möller and Shapiro (2002) calculated the unbalanced flow in the simulation of Hurricane Opal of 1995 and

found that the unbalanced flow extended far outside the eyewall region in the upper troposphere. They also demonstrated that the asymmetric balance (AB) formulation overestimated the spinup in the inner core region. For this reason, we directly use momentum and thermodynamic budget equations to assess the contributions of the eddy fluxes associated with the asymmetries to the tendencies of radial and tangential winds and potential temperature.

In cylindrical coordinates with an origin at the center of the TC, we can write the equations describing the eddy contributions as follows:

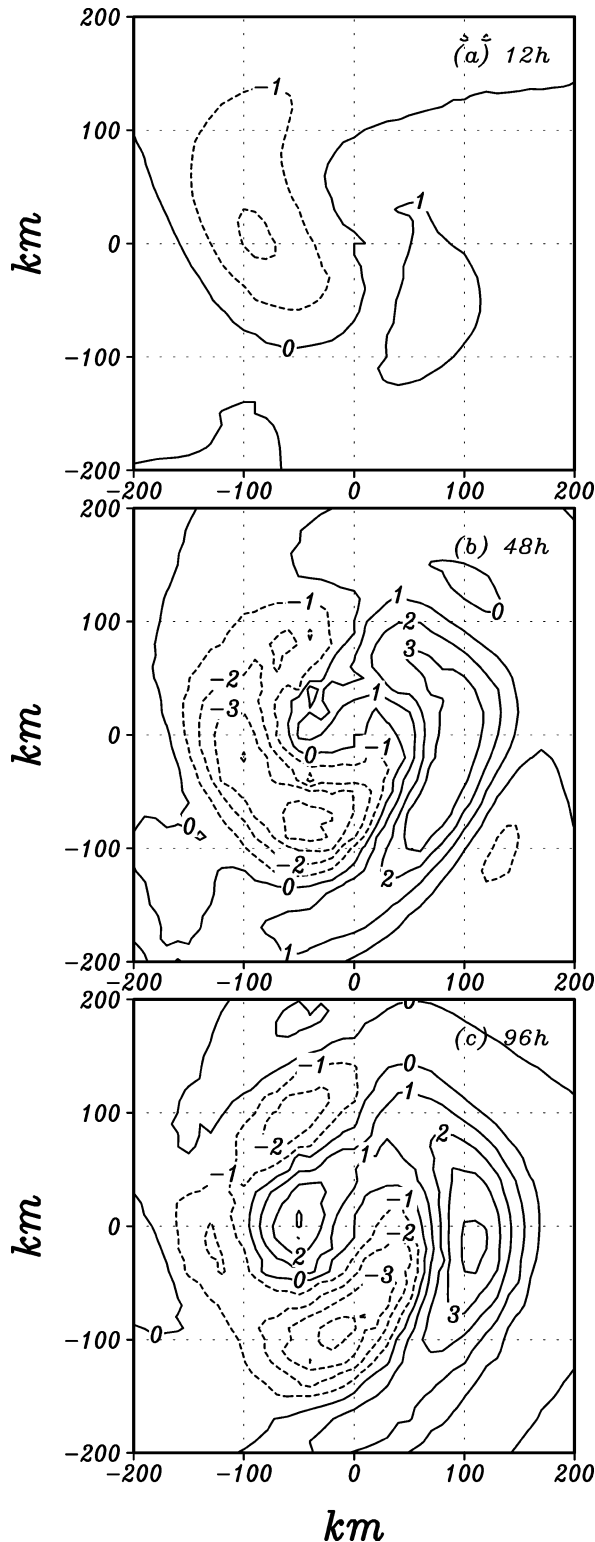


FIG. 7. Asymmetric vertical motion fields at level 9 (585 mb) after 12-, 48-, and 96-h integration in E3. The unit for vertical motion in σ coordinates is $10^{-5} \text{ Pa s}^{-1}$.

$$\left(\frac{\partial \bar{u}}{\partial t}\right)_{\text{eddy}} = -\left(\frac{\overline{u'^2} - \overline{v'^2}}{r} + \frac{\partial \overline{u'^2}}{\partial r} + \frac{\partial \overline{u' \omega'}}{\partial p}\right), \quad (1)$$

$$\left(\frac{\partial \bar{v}}{\partial t}\right)_{\text{eddy}} = -\left(\frac{2\overline{u'v'}}{r} + \frac{\partial \overline{u'v'}}{\partial r} + \frac{\partial \overline{v' \omega'}}{\partial p}\right) \quad (2)$$

$$\left(\frac{\partial \bar{\theta}}{\partial t}\right)_{\text{eddy}} = -\left(\frac{\overline{u'\theta'}}{r} + \frac{\partial \overline{u'\theta'}}{\partial r} + \frac{\partial \overline{\theta' \omega'}}{\partial p}\right), \quad (3)$$

where t , r , λ , and p are time, radius, azimuth, and pressure, respectively; \bar{u} , \bar{v} , and $\bar{\theta}$ are the azimuthal mean radial and tangential winds and potential temperature; and u' , v' , w' , and θ' are the asymmetric radial, tangential, and vertical winds, and potential temperature, respectively. Equations (1)–(3) indicate that the asymmetries can affect the tendencies of the tangential and radial winds and the potential temperature of the mean symmetric circulation through the terms on the right-hand side.

In order to evaluate the effects of the eddy fluxes on the tendencies of the mean tangential and radial winds and potential temperature, the model output is interpolated to a cylindrical coordinate system centered on the TCs. Since some uncertainty may be introduced as a result of inaccuracies of the center locations at any one time, terms associated with the eddy fluxes are calculated each hour and averaged over the period from 24 to 96 h for the three experiments. The time-averaged calculations are more likely to represent the persistent physical processes as compared to calculations from a single time step.

Figure 8 shows the 72-h-averaged contributions from the asymmetric circulation to the tendency of the mean radial wind in E1, E2, and E3, respectively. The contributions, primarily confined to the vicinity of the RMW, affect TC intensity in two ways. First, a positive center is located around the RMW near the surface that tilts outward with height, and a center of negative tendencies appears at about 750 mb. Since the transition of the low-level inflow and outflow occurs at 850 mb (Fig. 1c), the tendency of the radial wind indicates that the inflow and outflow are reduced because of the eddy momentum flux. In other words, an extra radial circulation is induced that is contrary to the mean secondary radial circulation, as indicated schematically in the figure. Second, as shown in Fig. 8, the eddy flux associated with the asymmetric circulation induces significant negative tendencies in the upper troposphere. Since the locations of the negative tendencies coincide with the outflow layer (see Fig. 1c), these negative tendencies effectively reduce the mean outflow from the eyewall in the upper troposphere. Comparing Fig. 8 with Fig. 4 suggests that the mean radial wind tendency associated with the induced asymmetric TC circulation directly affects the mean radial circulation, especially in the outflow layer, since the changes in the radial winds are

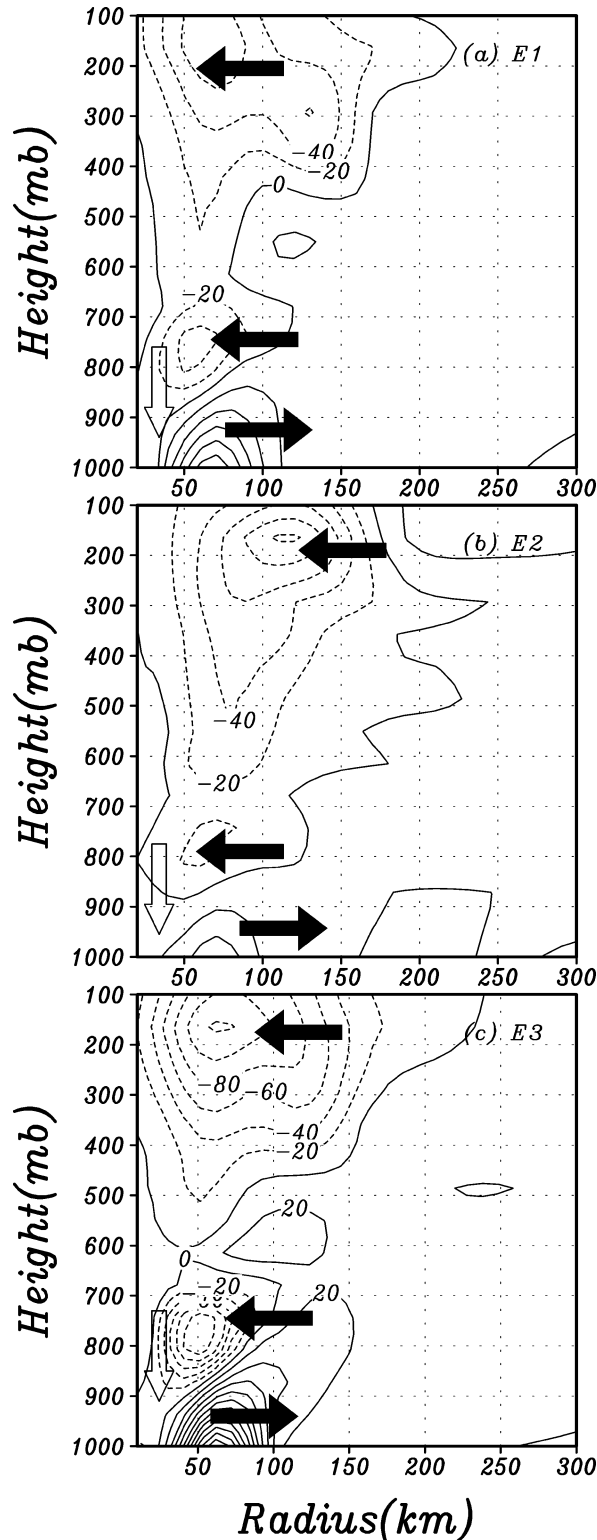


FIG. 8. Vertical cross section of the 72-h azimuthal contribution of the asymmetric circulation to the mean radial wind tendency, which is calculated from 24 to 96 h. Contour intervals are $20 \text{ m s}^{-1} \text{ day}^{-1}$. The solid arrows schematically show the directions of the induced mean radial flows, and the open arrows show the implied mean downward motion.

roughly similar to the patterns of the tendencies (Fig. 8).

Figure 9 shows the 72-h-averaged contributions from the induced asymmetries to the mean tangential wind tendency. Significant negative centers of the tendencies are found at lower levels and upper levels. When compared to Fig. 1b, the low-level negative centers are roughly located inside the core of the maximum winds while the upper-level negative centers are within the core, indicating that the negative tendencies reduce the TC intensity. In addition, the reduction of the tangential winds at the lowest level leads to a decrease of the surface fluxes that are crucial to maintaining TC intensity (Emanuel 1988). The mean tangential wind tendency is not uniform in the vertical. The vertical distribution suggests that, if we consider only the influence of the eddy mean azimuthal momentum fluxes, the tangential winds tend to be reduced at lower and upper levels, while less reduction or enhancement occurs at middle levels. The tangential wind changes shown in Fig. 3 are consistent with the tangential wind tendencies in that there is a relatively smaller reduction at middle levels, suggesting a direct influence of the eddy momentum flux on the mean tangential wind. Figure 10 shows the evolution of the tendency of mean tangential wind at 900 mb in each case. Comparing this figure with Fig. 2 indicates that the intensity changes relative to E0 occur after the onset of the eddy-induced tendencies. The evolution of the tendencies of the mean radial wind is similar (not shown).

Although the above discussion suggests that the eddy fluxes can directly affect the mean tangential and radial winds, tendencies associated with the symmetric circulation can counteract the effects of the eddy fluxes. In order to estimate the tendencies of the mean tangential and radial winds resulting from symmetric TC circulation, these tendencies are written as

$$\left(\frac{\partial \bar{v}}{\partial t}\right)_{\text{eddy}} = -\left(\frac{\partial r \bar{u} \bar{v}}{r \partial r} + \frac{\partial \bar{v} \bar{\omega}}{\partial p}\right) - \left(f \bar{u} + \frac{\bar{u} \bar{v}}{r}\right) + \bar{F}_\lambda + \bar{D}_\lambda, \quad (4)$$

$$\left(\frac{\partial \bar{u}}{\partial t}\right)_{\text{mean}} = -\left(\frac{\partial r \bar{u}^2}{r \partial r} + \frac{\partial \bar{u} \bar{\omega}}{\partial p}\right) + \left(f \bar{v} + \frac{\bar{v}^2}{r}\right) + \bar{F}_r + \bar{D}_r, \quad (5)$$

where $\bar{\phi}$ is mean geopotential and \bar{F}_r , \bar{F}_λ , \bar{D}_r , and \bar{D}_λ are mean friction and diffusion in radial and tangential directions. For convenience, the terms in (4) and (5) are organized into three groups. The terms in the first and second pairs of parentheses on the right-hand side of (4) and (5) are called the horizontal and vertical advection (HVA) and Coriolis and pressure gradient (CPG) terms, respectively, while the last two terms are friction and diffusion (FRD). The total contribution (TOT) is calculated as the sum of these terms. In order

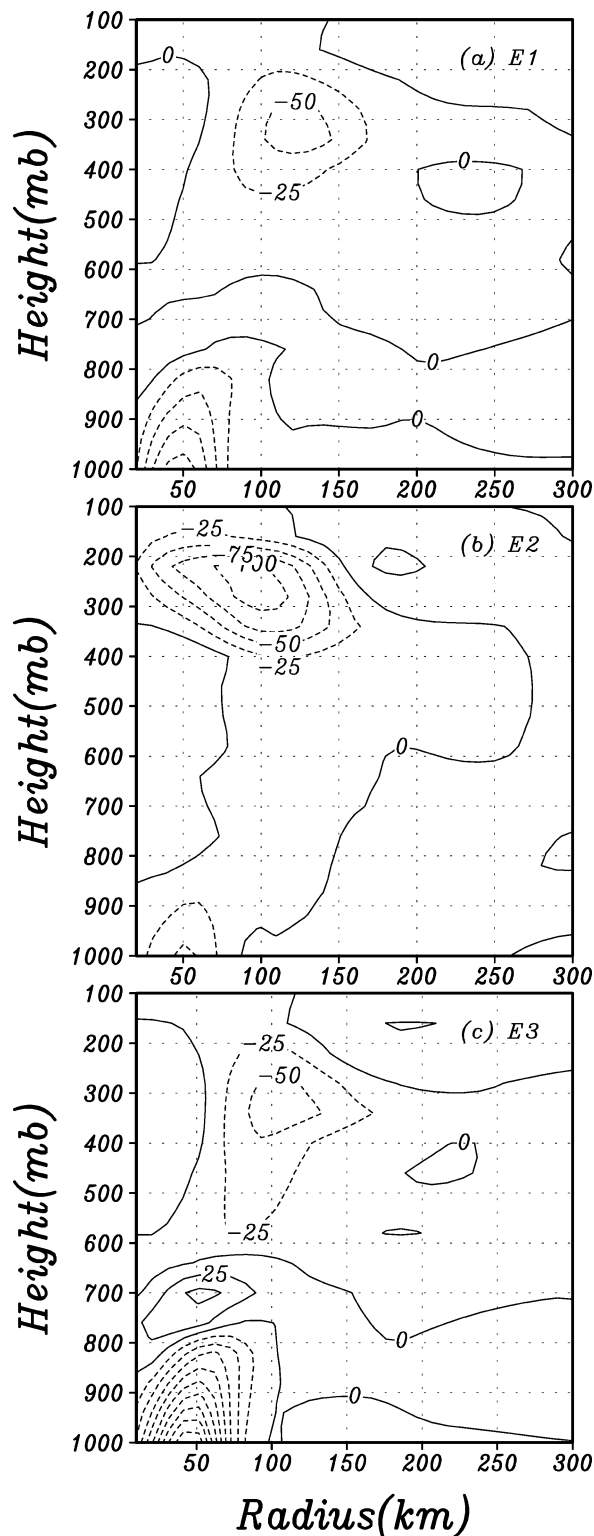


FIG. 9. As in Fig. 8 but for the eddy contribution to the mean tangential wind tendency. Contour intervals are $25 \text{ m s}^{-1} \text{ day}^{-1}$.

to estimate the contributions of the mean circulation caused by the environmental influences, the mean tendency terms in (4) and (5) are examined relative to E0. Since the patterns of these contributions in E1, E2, and E3 are very similar, we show only the calculations for E2.

Figure 11 shows the resulting changes in the mean radial wind tendency calculated with (5) compared with E0. The change in the CPG contribution (Fig. 11b), which indicates the imbalance between the Coriolis force and pressure gradient in the TC inner region, tends to be approximately balanced by the HVA and FRD contributions (Fig. 11a). The changes in these contributions occur mainly in the core region within a radius of 150 km. The largest tendency changes caused by the symmetric circulation are primarily confined to the inflow layer and inside of the RMW. In the TOT tendency change (Fig. 11d), positive values are found inside of the RMW at lower and upper levels. The positive contributions in the middle and upper troposphere tend to enhance the outflow, while in the lower boundary layer the positive changes tend to reduce the low-level inflow. As a result, the tendencies associated with the mean TC circulation (relative to E0) act to reduce the low-level inflow, while at upper levels they act to enhance the outflow and oppose the effects of the eddies (Fig. 11d).

The contributions of the mean circulation (relative to E0) to the changes in tangential wind [Eq. (4)] are shown in Fig. 12. The change in the FRD contribution (Fig. 12c) is primarily confined to the boundary layer inside of the eye and the change in HVA (Fig. 12a) tends to balance most of the change in CPG (Fig. 12b). The total tendency change resulting from the symmetric circulation change (Fig. 12d) results in an increase of the mean tangential wind at all levels in the vicinity of the RMW, suggesting that the effects of the mean circulation tend to counteract the influence of the eddies and that the eddies are primarily responsible for the reduced tangential winds.

While the results in Figs. 9b and 12d are in qualitative agreement with the tangential wind changes in Fig. 3b, quantitative assessment is not attained. This problem also occurs with the radial flow (Figs. 4b, 8b, and 11d). A key source of uncertainty is in the calculation of the tendencies resulting from the symmetric TC circulation change. These tendencies are calculated from a symmetric circulation that is interpolated onto a cylindrical grid based upon the estimated center position. Because of the coarse horizontal resolution, if a 1% error in the mean tangential wind speed (50 m s^{-1}) at the RMW (100 km) occurs, then this 0.5 m s^{-1} error yields an error in \bar{v}^2/r of $43.2 \text{ m s}^{-1} \text{ day}^{-1}$. A similar error in the asymmetric wind speed produces a relatively smaller error in the contributions of eddies since the asymmetric wind speed is generally much smaller than the symmetric wind speed. The temporal averaging helps to minimize the error at any one time, but sufficient error

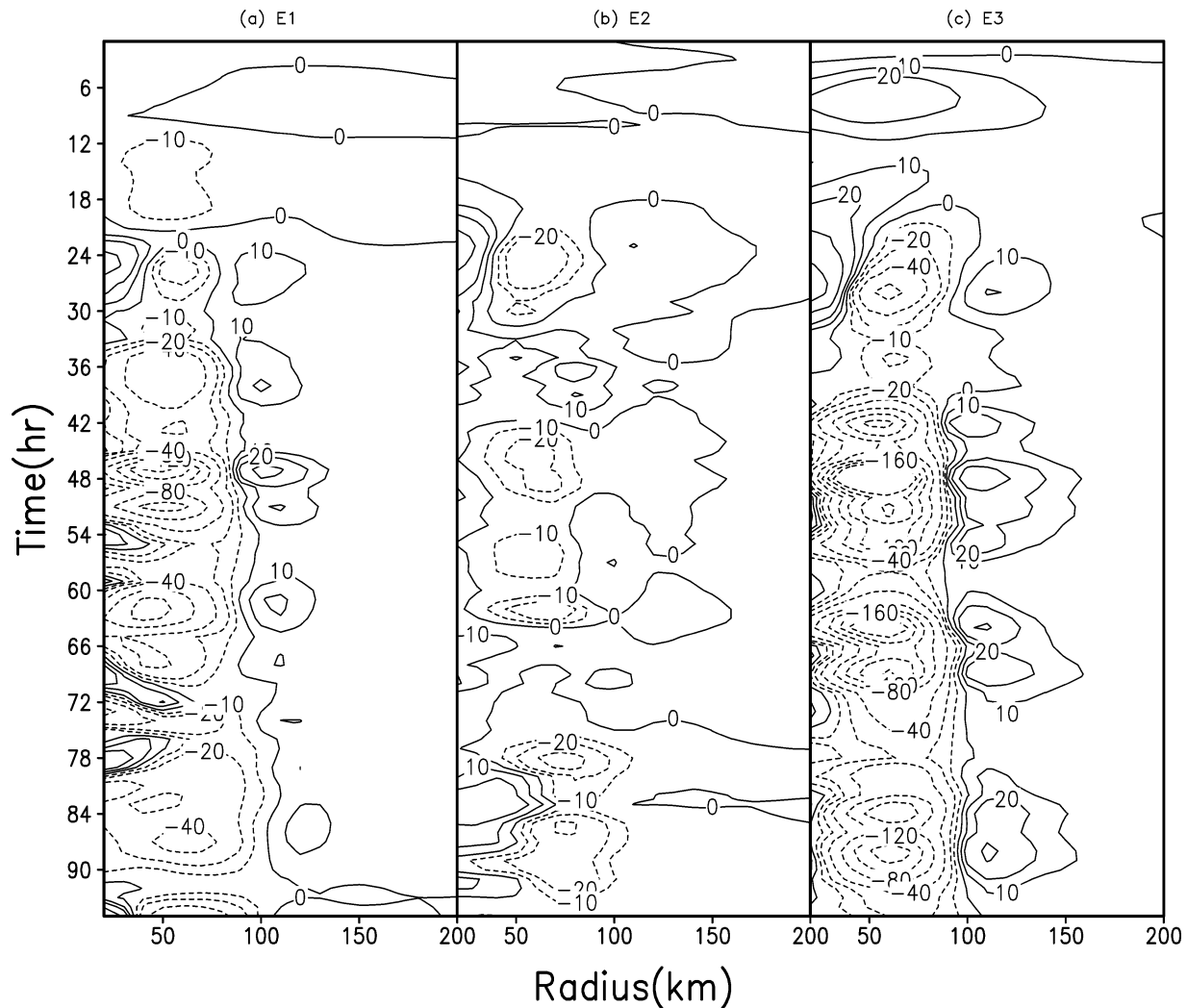


FIG. 10. Tendencies of mean tangential wind associated with eddy fluxes at 900 mb. Contours are 0, ± 10 , ± 20 , ± 40 , ± 80 , ± 120 , ± 160 , and ± 200 $\text{m s}^{-1} \text{day}^{-1}$.

exists such that the results are less meaningful quantitatively but are still qualitatively valid.

It is generally believed that most hurricanes fail to reach their MPI primarily because of wind-induced sea surface cooling, downdrafts, or the inhibiting effect of vertical wind shear. Previous studies (Gray 1968; Anthes 1972, 1982; Frank and Ritchie 2001) suggested that shear inhibits intensification through differential advection of the upper warm anomaly from the low-level circulation, thereby raising the pressure at lower levels according to hydrostatic balance. Figure 13 shows the temperature deviations in E1, E2, and E3 from that in E0 at 96 h, respectively. The temperature changes in the eye are qualitatively similar in all three cases, with the air in the eye warmer at lower and middle levels and cooler at upper levels. Since no environmental shear is involved in cases E2 and E3, these temperature deviations are not caused by the differential advection associated with vertical shear. Figure 14 shows the ten-

dencies of the mean potential temperature caused by the asymmetries. Comparing Fig. 14 with Fig. 13 suggests that the temperature deviations are not the direct result of the mean eddy heat flux on the right-hand side of (3). In Fig. 14, negative tendencies in the eyewall region are apparent in all three cases, but Fig. 13 indicates that these negative temperature tendencies do not significantly modify the temperature in the eyewall.

We have shown that the eddy momentum fluxes act to weaken the tangential circulation and are generally opposed by the contributions from the symmetric circulation. Since the warm core is, to first order, in thermal wind balance with the tangential circulation (Smith 1980) and the latter is reduced most strongly at upper levels (Figs. 3 and 9) as a result of the eddy momentum fluxes, it follows that the tangential circulation is shallower and that the core of the warm anomaly should be lower. This result, in turn, leads to an increase in the hydrostatic pressure at the surface in the eye.

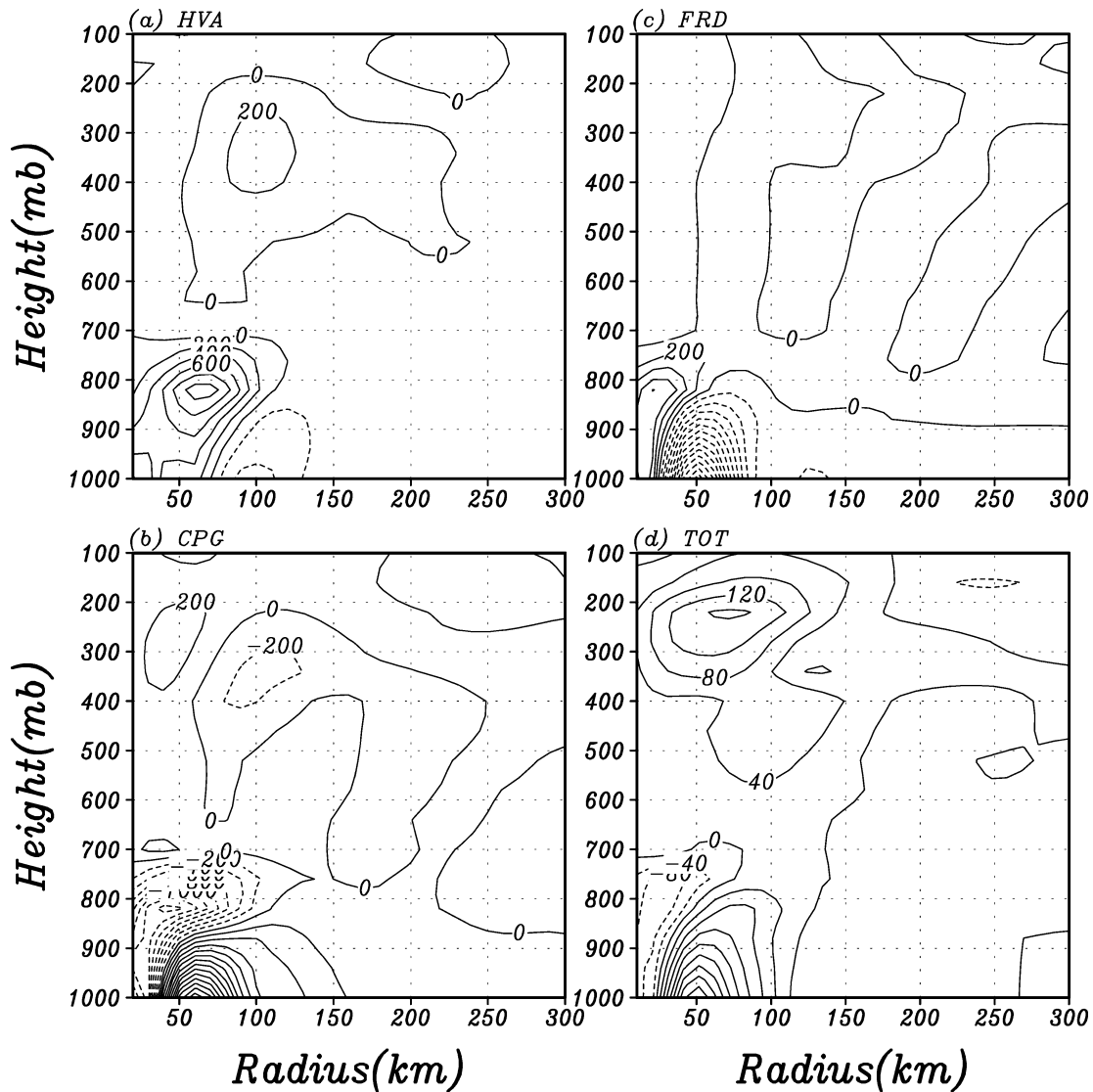


FIG. 11. Difference of mean radial wind tendencies resulting from the mean TC circulation change, which is averaged from 24 to 96 h (see the text for each term) between E2 and E0. Contours are $200 \text{ m s}^{-1} \text{ day}^{-1}$ for (a), (b), and (c), but $20 \text{ m s}^{-1} \text{ day}^{-1}$ for (d).

5. Discussion

Previous studies on the effects of TC rainbands have focused on the weakening of eyewall convection caused by downdrafts. Powell (1990) found that mesoscale descent and occasional convective-scale penetrative downdrafts are present on the inward side of outer convective rainbands and tend to transport low θ_e air into the boundary layer. Since the Kuo cumulus scheme does not include convective downdrafts, their effects are not responsible for the weakening in our experiments. Previous studies (e.g., Frank and Ritchie 2001) have also suggested that ventilation of the warm core by shear can increase the TC central pressure. However, in this study even the case with only a uniform flow experiences weakening as asymmetries develop, suggesting

that this effect is not responsible for the weakening in our experiments.

Recent observational (e.g., Reasor et al. 2000) and numerical (Chen and Yau 2001; Wang 2002a,b; Chen et al. 2003) studies suggest that eyewall asymmetries are a common feature for tropical cyclones. It has been well demonstrated that precipitation in the eyewall tends to occur on the downshear-left side (Frank and Ritchie 1999, 2001; Reasor et al. 2000). As shown in Fig. 6, the positive maxima of eyewall PV generally occur ahead and to the right of the storm motion vector, suggesting that these eyewall asymmetries, induced by large-scale environmental influences, mainly exhibit characteristics of quasi-stationary wavenumber-1 vortex Rossby waves. Smith and Montgomery (1995) attributed the

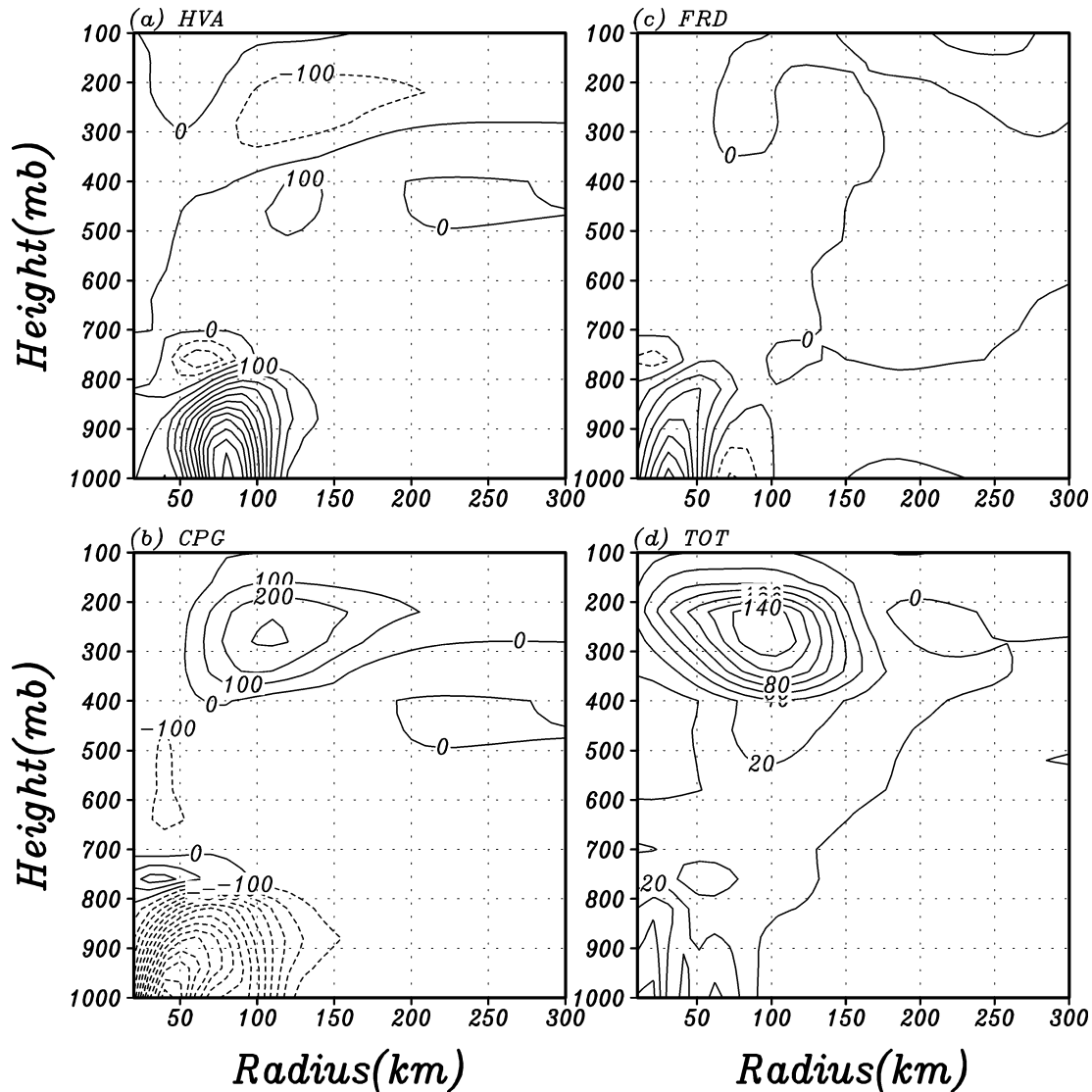


FIG. 12. Difference of mean tangential wind tendencies resulting from the mean TC circulation change between E2 and E0, which is averaged from 24 to 96 h (see the text for each term). Contours are $100 \text{ m s}^{-1} \text{ day}^{-1}$ for (a), (b), and (c), but $20 \text{ m s}^{-1} \text{ day}^{-1}$ for (d).

dominance of low-azimuthal-wavenumber asymmetries, especially wavenumber 1, to a wavenumber selection mechanism that preferentially damps the high-wavenumber asymmetries. This study has demonstrated that the eddy momentum fluxes associated with environmentally induced eyewall asymmetries weaken the tangential and radial flows of the mean TC circulation, especially in the inflow and outflow layers. In other words, these eyewall asymmetries reduce the kinetic energy of the mean vortex flow.

Figure 15 shows the asymmetric wind fields (left panels) associated with the contribution of the eddy fluxes to the tangential wind in E3 at 72 h. At 900 mb (lower panels), significant deceleration is associated with a pair of gyres centered on the RMW. At 350 mb (upper pan-

els), the negative values that extend as far as 200 km from the center are related to relatively weak asymmetric flows. The environmentally induced asymmetries are quasi-stationary, and their coherent structure is primarily driven by diabatic heating (Wang 2002a; Chen and Yau 2001). They tend to transport energy to the outside of the eyewall due to their nature of the vortex Rossby waves (Montgomery and Kallenbach 1997).

The calculations shown in Figs. 8 and 9 also suggest that the eyewall asymmetries obtain some kinetic energy from the mean vortex through the eddy fluxes. Wang (2002b) in a kinetic energy budget analysis suggested that the energy conversion from the mean vortex is also important to the energetics of eyewall asymmetries. After breaking the barotropic and baroclinic conversions

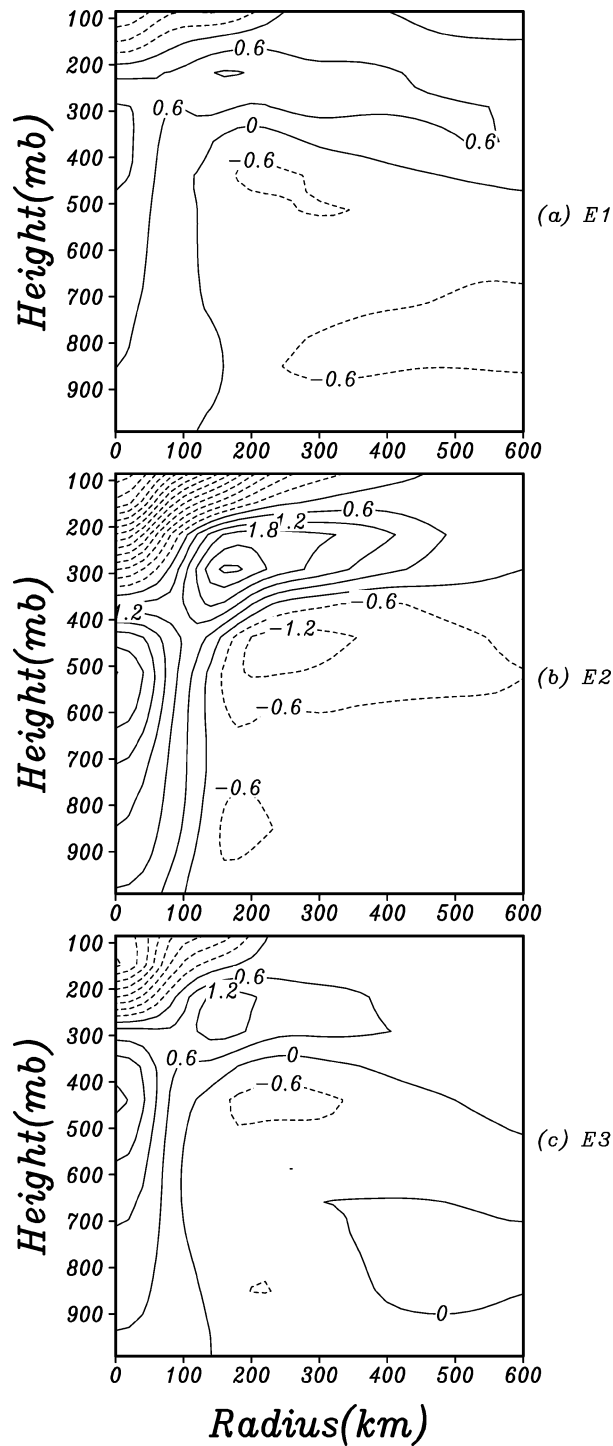


FIG. 13. Deviation of temperature in (a) E1, (b) E2, and (c) E3 from that in E0 at 96 h. The intervals are 0.6°C .

into terms associated with the tangential and radial flows of the mean vortex, respectively, he further found that the energy conversion is closely associated with the mean vortex flow. In the outflow layer, the barotropic and baroclinic conversions associated with the tangen-

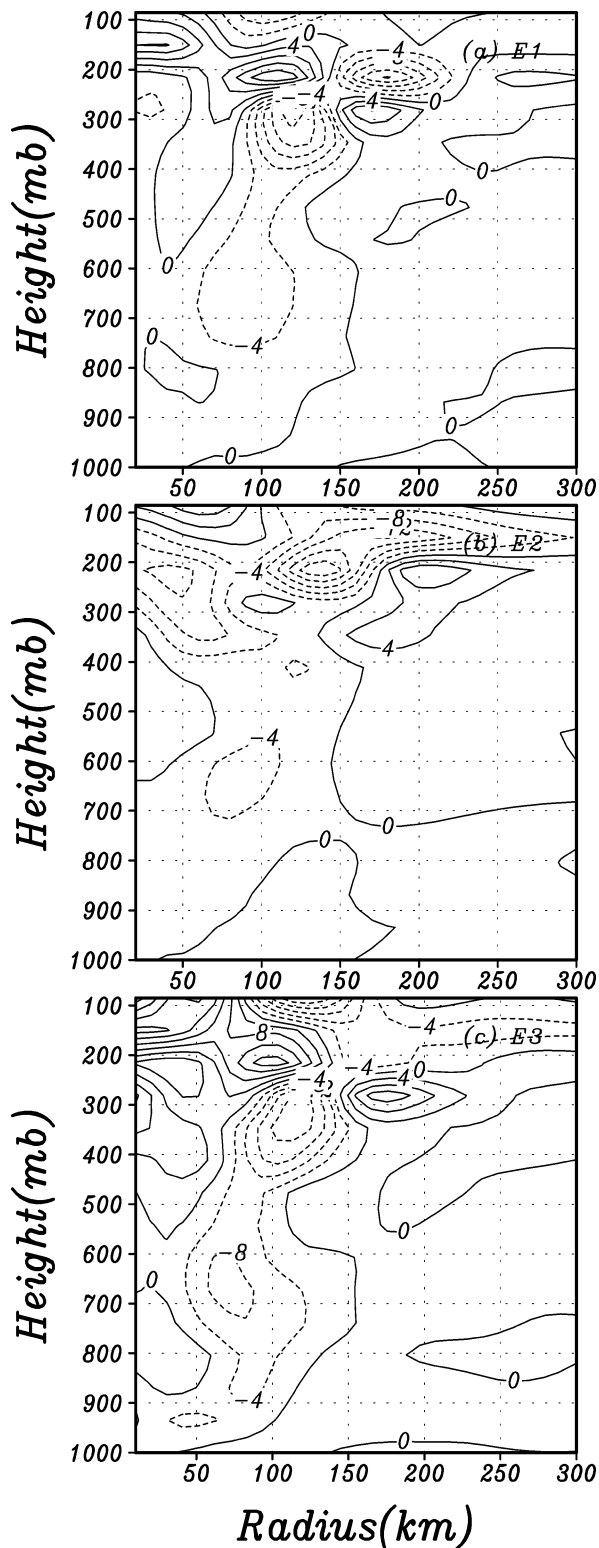


FIG. 14. As in Fig. 8 but for the eddy contribution to the mean potential temperature. Contour intervals are 4 K day^{-1} .

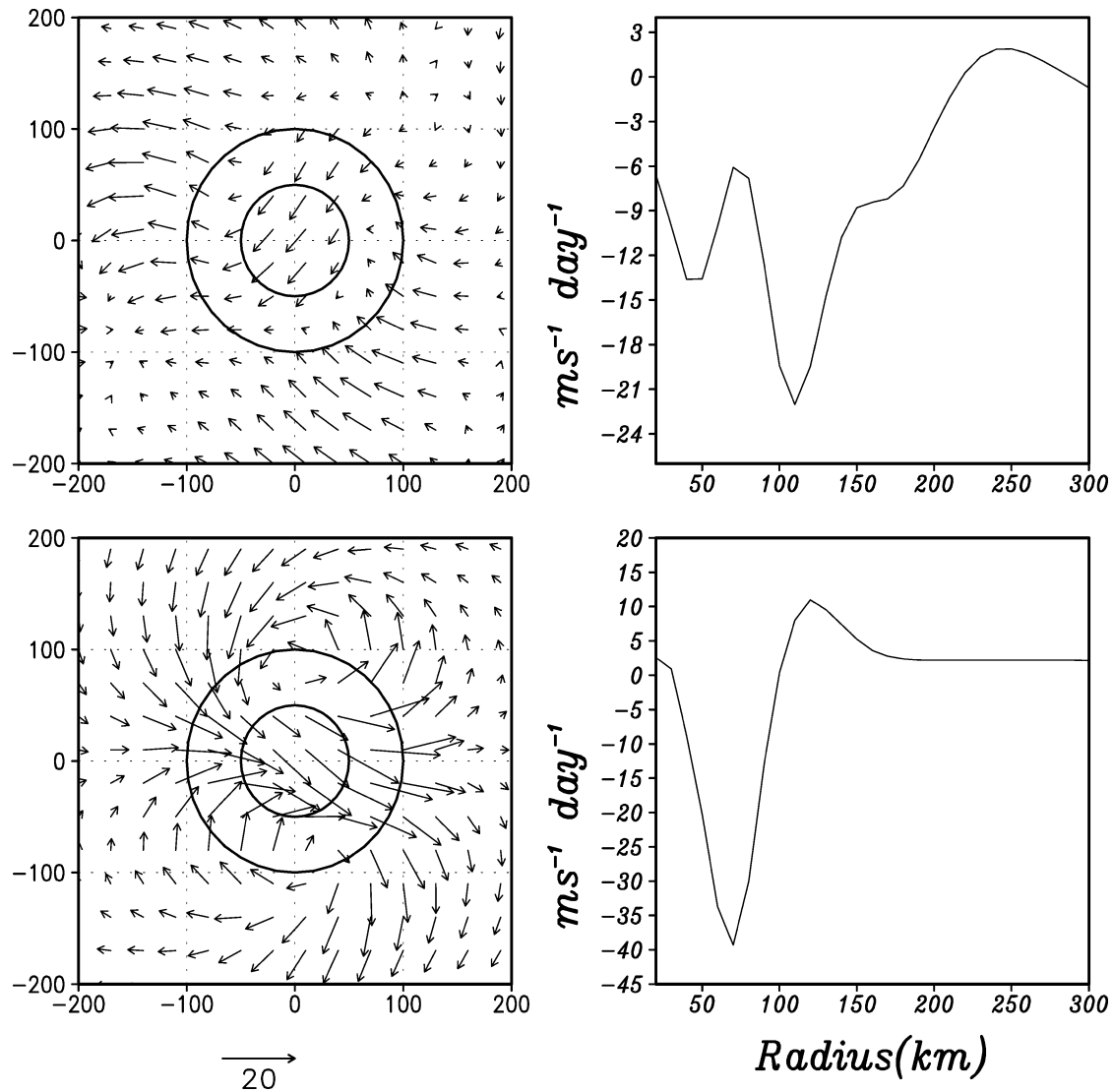


FIG. 15. (left) Asymmetric components of the winds and (right) the tendency of mean tangential wind associated with horizontal eddy momentum flux at 350 and 900 mb in E3 at 72 h.

tial flow of the mean vortex are important energy sources for eyewall asymmetries. In the lower troposphere, on the other hand, eyewall asymmetries receive their energy through the barotropic term associated with the mean radial flow and the baroclinic terms associated with both mean tangential and radial flows, while eyewall asymmetries lose their energy to the mean circulation through the barotropic conversion associated with the mean tangential. As shown in Figs. 8 and 9, significant deceleration of mean tangential wind occurs in the layers with strong mean radial flows, while the low-to-midlevel weak deceleration or acceleration is associated with the region with weak mean radial flow. Nolan and Farrell (1999) also found that neglecting the radial inflow terms greatly overestimates the potential for transient growth or even destabilizes the vortex completely.

Based on this study, the inhibiting effect of environmental influences can be summarized as follows. Interaction between the TC symmetric circulation and environmental influences leads to the development of quasi-stationary symmetries in the vicinity of the TC eyewall, which are dominated by the wavenumber-1 component. The eyewall asymmetries extract a small portion of their kinetic energy from the mean vortex, decelerating mean tangential and radial flows, particularly in the inflow and outflow layers in the vicinity of the eyewall. The corresponding changes in the TC symmetric circulation tend to balance the deceleration effect. In this regard, an analogy to Lenz's law in classical electrodynamics may be drawn as follows. The effects of the eddy fluxes (analogous to a change in magnetic field) lead to a change in the symmetric circulation (the induced current) that produces forces that oppose the

eddy fluxes. The net effect is a moderate weakening of the TC mean tangential and radial winds in the inflow and outflow layers. The reduced radial wind can be viewed in terms of an anomalous secondary radial circulation with inflow in the upper troposphere and outflow in the lower troposphere, weakening the mean secondary radial circulation.

6. Conclusions

Weakening of a TC resulting from the large-scale influences has been observed in many previous studies (e.g., Peng et al. 1999; Frank and Ritchie 1999, 2001; Wu 1999). In order to understand this phenomenon better, idealized experiments are designed to include uniform environmental flow, the beta effect, and vertical shear. The effects of convective downdrafts on TC intensity are excluded by using a relatively coarse-resolution model with a cumulus scheme that does not include downdrafts. The simulated effects of the environmental influence on TC intensity are very similar to the previous studies (Peng et al. 1999; Frank and Ritchie 1999, 2001; Wu 1999), but an alternative explanation for these effects is provided. In response to the environmental influence, significant asymmetries develop, primarily in the wavenumber-1 component, with their structure resembling TC spiral bands. The effects of the induced asymmetries on intensity are investigated in the context of the associated eddy fluxes of momentum and heat.

Simulation results suggest that the inhibiting effect of the environmental influences on TC intensity results from induced quasi-stationary asymmetries in the inner core region. The eyewall asymmetries interact with the mean vortex through eddy momentum fluxes and partially extract their kinetic energy from the mean vortex, leading to the weakening of the mean TC tangential and radial winds. The reduced radial winds are associated with an anomalous secondary radial circulation, with inflow in the upper troposphere and outflow in the lower troposphere, that opposes the mean secondary radial circulation. Changes in the tendencies associated with the TC symmetric circulation tend to counteract the effects of the core asymmetries so that the rate of spin-down of the vortex is much slower than that implied by the tendencies associated with the asymmetries. The reduction of the tangential winds lowers the height of the warm anomaly through thermal wind balance, thereby increasing the minimum central pressure relative to the case without environmental influence.

The numerical experiments in this study focus on the effects of the asymmetries induced by simple large-scale flows. In a recent high-resolution study Chen and Yau (2003) found that the eddies associated with eyewall asymmetries not only decelerate the tangential wind at the RMW but also accelerate the wind inside the RMW during the intensification stage. That means the interaction between the eyewall asymmetries and the mean

vortex flow can also lead to the eyewall contraction. However, the eyewall contraction in the present study is poorly simulated due to the coarse horizontal resolution. In addition, the environmental effects are designed to be moderate and idealized in order to facilitate our analysis, but may underestimate the effects that might occur in the presence of other physical processes. For this reason, further investigation of the various physical mechanisms responsible for TC intensity change is needed using high-resolution simulations with more sophisticated model physics.

Acknowledgments. The authors gratefully acknowledge Dr. Michael Montgomery, Dr. Kerry Emanuel, and two anonymous reviewers for their valuable comments. Acknowledgment is also made to Dr. Yuqing Wang for letting us use his model and to Dr. R. Kadar (NASA/HQ) for his support of this research under the NASA CAMEX-4 research program.

REFERENCES

- Anthes, R. A., 1972: The development of asymmetries in a three-dimensional numerical model of tropical cyclones. *Mon. Wea. Rev.*, **100**, 461–476.
- , 1982: *Tropical Cyclones: Their Evolution, Structure and Effects*. Meteor. Monogr., No. 41, Amer. Meteor. Soc., 208 pp.
- Betts, A. K., and M. Miller, 1986: A new convective adjustment scheme. Part II: Single column tests using GATE waves, BOMEX, ATEX and arctic air-mass data sets. *Quart. J. Roy. Meteor. Soc.*, **112**, 693–709.
- Bosart, L. E., C. S. Velden, W. E. Bracken, J. Molinari, and P. G. Black, 2000: Environmental influences on the rapid intensification of Hurricane Opal (1995) over the Gulf of Mexico. *Mon. Wea. Rev.*, **128**, 322–352.
- Challa, M., and R. L. Pfeffer, 1980: Effects of eddy fluxes of angular momentum on the model hurricane development. *J. Atmos. Sci.*, **37**, 1603–1618.
- , —, Q. Zhao, and S. W. Chang, 1998: Can eddy fluxes serve as a catalyst for hurricane and typhoon formation? *J. Atmos. Sci.*, **55**, 2201–2219.
- Chen, Y., and M. K. Yau, 2001: Spiral bands in a simulated hurricane. Part I: Vortex Rossby wave verification. *J. Atmos. Sci.*, **58**, 2128–2145.
- , and —, 2003: Asymmetric structure in a simulated land-falling hurricane. *J. Atmos. Sci.*, **60**, 2294–2312.
- , G. Brunet, and M. K. Yau, 2003: Spiral bands in a simulated hurricane. Part II: Wave activity diagnostics. *J. Atmos. Sci.*, **60**, 1239–1255.
- Eliassen, A., 1952: Slow thermally or frictionally controlled meridional circulation in a circular vortex. *Astrophys. Norv.*, **5**, 19–60.
- Emanuel, K. A., 1988: The maximum intensity of hurricanes. *J. Atmos. Sci.*, **45**, 1143–1155.
- Enagonio, J., and M. T. Montgomery, 2001: Tropical cyclogenesis via convectively forced vortex Rossby waves in a shallow water primitive equation model. *J. Atmos. Sci.*, **58**, 685–705.
- Frank, W. M., and E. A. Ritchie, 1999: Effects on environmental flow upon tropical cyclone structure. *Mon. Wea. Rev.*, **127**, 2044–2061.
- , and —, 2001: Effects of vertical wind shear on the intensity and structure of numerically simulated hurricanes. *Mon. Wea. Rev.*, **129**, 2249–2269.
- Gall, R., J. Tuttle, and P. Hildbrand, 1998: Small-scale spiral bands observed in Hurricane Andrew, Hugo and Erin. *Mon. Wea. Rev.*, **126**, 1749–1766.

- Gray, W. M., 1968: Global view of the origin of tropical disturbances and storms. *Mon. Wea. Rev.*, **96**, 669–700.
- Jones, S. C., 1995: The evolution of vortices in vertical shear. Part I: Initially barotropic vortices. *Quart. J. Roy. Meteor. Soc.*, **121**, 821–851.
- Jordan, C. L., 1952: On the low-level structure of typhoon eye. *J. Meteor.*, **9**, 285–290.
- Jorgensen, D. P., 1984: Mesoscale and convective-scale characteristics of mature hurricanes. Part III: Inner core structure of Hurricane Allen (1980). *J. Atmos. Sci.*, **41**, 1287–1311.
- Kuo, H. C., R. T. Williams, and J.-H. Chen, 1999: A possible mechanism for the eye rotation of Typhoon Herb. *J. Atmos. Sci.*, **56**, 1659–1673.
- Kuo, H. L., 1974: Further studies of the parameterization of the influence of cumulus convection on large-scale flow. *J. Atmos. Sci.*, **31**, 1232–1240.
- Lewis, B. M., and H. F. Hawkins, 1982: Polygonal eyewalls and rainbands in hurricanes. *Bull. Amer. Meteor. Soc.*, **63**, 1294–1300.
- Louis, J. F., 1979: A parametric model of vertical eddy fluxes in the atmosphere. *Bound.-Layer Meteor.*, **17**, 746–756.
- May, P. T., and G. J. Holland, 1999: The role of potential vorticity generation in tropical cyclone rainbands. *J. Atmos. Sci.*, **56**, 1224–1228.
- Melander, M. V., J. C. McWilliams, and N. J. Zabusky, 1987: Axisymmetrization and vorticity-gradient intensification of an isolated two-dimensional vortex through filamentation. *J. Fluid Mech.*, **178**, 137–159.
- Molinari, J., and D. Volaro, 1990: External influences on hurricane intensity. Part II: Vertical structure and response of the hurricane vortex. *J. Atmos. Sci.*, **47**, 1902–1918.
- Möller, J. D., and M. T. Montgomery, 1999: Vortex Rossby waves and their influence on hurricane intensification in a barotropic model. *J. Atmos. Sci.*, **56**, 1674–1687.
- , and —, 2000: Tropical cyclone evolution via potential vorticity anomalies in a three-dimensional balanced model. *J. Atmos. Sci.*, **57**, 3366–3387.
- , and L. S. Shapiro, 2002: Balanced contributions to the intensification of Hurricane Opal as diagnosed from a GFDL model forecast. *Mon. Wea. Rev.*, **130**, 1866–1881.
- Montgomery, M. T., and R. J. Kallenbach, 1997: A theory for vortex Rossby-waves and its application to spiral bands and intensity changes in hurricanes. *Quart. J. Roy. Meteor. Soc.*, **123**, 435–465.
- , and J. Enagonio, 1998: Tropical cyclogenesis via convectively forced vortex Rossby waves in a three-dimensional quasigeostrophic model. *J. Atmos. Sci.*, **55**, 3176–3207.
- Nolan, D. S., and B. F. Farrell, 1999: The intensification of two-dimensional swirling flows by stochastic asymmetric forcing. *J. Atmos. Sci.*, **56**, 3937–3962.
- Peng, M. S., B.-F. Jeng, and R. T. Williams, 1999: A numerical study on tropical cyclone intensification. Part I: Beta effect and mean flow effect. *J. Atmos. Sci.*, **56**, 1404–1423.
- Persing, J., M. T. Montgomery, and R. E. Tuleya, 2002: Environmental interactions in the GFDL hurricane model of Hurricane Opal. *Mon. Wea. Rev.*, **130**, 298–317.
- Pfeffer, R. L., 1958: Concerning the mechanics of hurricanes. *J. Meteor.*, **15**, 113–120.
- Powell, M., 1990: Boundary layer structure and dynamics in outer hurricane rainbands. Part II: Downdraft modification and mixed layer recovery. *Mon. Wea. Rev.*, **118**, 918–938.
- Reasor, P. D., M. T. Montgomery, F. D. Marks Jr., and J. F. Gamache, 2000: Low-wavenumber structure and evolution of the hurricane inner core observed by airborne dual-Doppler radar. *Mon. Wea. Rev.*, **128**, 1653–1680.
- Shapiro, L. J., 1983: Asymmetric boundary layer flow under a translating hurricane. *J. Atmos. Sci.*, **40**, 1984–1998.
- Shea, D. J., and W. M. Gray, 1973: The hurricane inner core region. I: Symmetric and asymmetric structure. *J. Atmos. Sci.*, **30**, 1544–1564.
- Simpson, R. H., 1952: Exploring the eye of typhoon “Marge” 1951. *Bull. Amer. Meteor. Soc.*, **33**, 286–298.
- Smagorinsky, J., S. Manabe, and J. L. Holloway Jr., 1965: Numerical results from a nine-level general circulation model of the atmosphere. *Mon. Wea. Rev.*, **93**, 727–768.
- Smith, G. B., and M. T. Montgomery, 1995: Vortex axisymmetrization: Dependence on azimuthal wave-number or asymmetric radial structure changes. *Quart. J. Roy. Meteor. Soc.*, **121**, 1615–1650.
- Smith, R. K., 1980: Tropical cyclone eye dynamics. *J. Atmos. Sci.*, **37**, 1227–1232.
- Wang, Y., 2002a: Vortex Rossby waves in a numerically simulated tropical cyclone. Part I: Overall structure, potential vorticity and kinetic energy budgets. *J. Atmos. Sci.*, **59**, 1213–1238.
- , 2002b: Vortex Rossby waves in a numerically simulated tropical cyclone. Part II: The role in tropical cyclone structure and intensity changes. *J. Atmos. Sci.*, **59**, 1239–1262.
- Willoughby, H. E., F. D. Marks Jr., and R. J. Feinberg, 1984: Stationary and moving convective bands in hurricanes. *J. Atmos. Sci.*, **41**, 3189–3211.
- Wu, L., 1999: Study of tropical cyclone motion with a coupled hurricane–ocean model. Ph.D. dissertation, Dept. of Meteorology, University of Hawaii, 212 pp.
- , and B. Wang, 2000: A potential vorticity tendency diagnostic approach for tropical cyclone motion. *Mon. Wea. Rev.*, **128**, 1899–1911.
- , and —, 2001a: Movement and vertical coupling of adiabatic baroclinic tropical cyclones. *J. Atmos. Sci.*, **58**, 1801–1814.
- , and —, 2001b: Effects of convective heating on movement and vertical coupling of tropical cyclones: A numerical study. *J. Atmos. Sci.*, **58**, 3639–3649.